ISSN 2394-3777 (Print)
ISSN 2394-3785 (Online)
Available online at www.ijartet.com
International Journal of Advanced Research Trends in Engineering and Technology (IJARTET)
Vol. 3, Special Issue 24, April 2016

ADAPTIVE COG-MAC SCHEME FOR COEXISTENCE OF IEEE 802.15.4 WITH OTHER INTERFERING SYSTEMS

Nirmal Kumar K[1],KalyanaSundaram P[2],Dr.T.Gnanasekaran[3]

[1]ME-Applied Electronics,[2]Professor/ECE ,[3]Professor/IT

[1&2]Nandha Engineering College, Erode-52,[3]RMK Engineering College,Chennai

***Abstract*—Energy efficiency has been the driving force behind the design of communication protocols for battery-constrained wireless sensor networks (WSNs). The energy efficiency and the performance of the proposed protocol stacks, however, degrade dramatically in case the low-powered WSNs are subject to interference from high-power wireless systems such as WLANs.In this paper we propose COG-MAC, a novel cognitive medium access control scheme (MAC) for IEEE 802.15.4-compliant WSNs that minimizes the energy cost for multihop communications, by deriving energy-optimal packet lengths and single-hop transmission distances based on the experienced interference from IEEE 802.11 WLANs. We evaluate COG-MAC by deriving a detailed analytic model for its performance and by comparing it with previous access control schemes. Numerical and simulation results show that a significant decrease in packet transmission energy cost, up to 66%, can be achieved in a wide range of scenarios, particularly under severe WLAN interference. COGMAC is, also, lightweight and shows high robustness against WLAN model estimation errors and is, therefore, an effective, implementable solution to reduce the WSN performance impairment when coexisting with WLANs.**

***Index Terms*—WSN, energy efficiency, cognitive networks, coexistence, IEEE 802.11, IEEE 802.15.4.**

I. INTRODUCTION

The increasing number of different wireless technologiessharing the open spectrum bands, such as the 2.4GHzISM band, demands for a rethinking of the protocols regulatingthe spectrum access. As the medium access control (MAC)schemes are carefully designed for one given technology, theyare not anymore able to achieve the objective of efficient and"fair" sharing of the wireless resources when operating underinterference from heterogeneous technologies.

In this paper we consider the specific case of the coexistenceof IEEE 802.11 wireless local area networks (WLANs) andIEEE 802.15.4-compliant wireless sensor networks (WSNs).Both technologies apply carrier sensing-based medium accesscontrol with collision avoidance. In addition, WSNs try tolocate the narrow frequency band with less harmful interferencefor their operations. Unfortunately, all these techniquesdo not avoid high interference and frequent packet losses in theWSN, which are mainly caused by the significantly differenttransmission bandwidths and powers of the two technologiescompeting for the same resource.As shown in [1], the

WLAN terminals operate in a relativelybroad channel and at a higher transmission power than WSNs.

Therefore, they are blind to the narrow-band, low-powered WSN transmissions, and do not defer channel access, due to the overlapping WSN packet transmission.

In all this, the WLAN transmissions remain basically unaffected by the low WSN interference, while WSN packets are lost. Fortunately, measurement results show that the WLAN traffic is rather bursty with long white spaces, when the channel is idle because all WLAN users are inactive [2]. Therefore, in order to maximize its performance, the WSN should be able to transmit in these long interference-free times, thus, being cognitive of the radio environment as imposed by

the WLAN activity.

In this paper we propose and evaluate a new CognitiveMAC (COG-MAC) protocol for wireless sensor networks,which extends the carrier sense-based MAC and aims atminimizing the energy loss due tounsuccessful transmissionsover the interfered channel. Our paper provides the following contributions.1)We give a characterization of the WLANchannel usage patterns as seen by the sensor nodes, takinginto account the nodes' limited channel estimation capabilities,and propose techniques for distributed WLAN usage pattern estimation.2) Based on these resulting WLAN channel usagecharacterization we design COG-MAC, that optimizes thepacket length and the transmission distance, and performsWLAN activity-aware channel access to ensure that WSNnodes transmit in the long

ISSN 2394-3777 (Print)
ISSN 2394-3785 (Online)
Available online at www.ijartet.com
International Journal of Advanced Research Trends in Engineering and Technology (IJARTET)
Vol. 3, Special Issue 24, April 2016

WLAN white space periods.3)We provide an accurate analytical model that describes theprobability of COG-MAC packet transmission success. We usethe model to optimize the WSN packet size and the single hopWSN transmission distance to minimize the normalizedenergy cost metric, which we define as the energy required tosuccessfully transmit and receive a unit of information over aunit of distance. 4) We show that all the basic componentsof COG-MAC are essential for achieving the objective ofenergy efficient communication, and COG-MAC, comparedto previous access schemes, reduces the normalized energycost up to 66%, and can significantly decrease the end-to-endenergy cost in a multihop WSN without increased delay.

The rest of the paper is organized as follows. Relatedwork is presented in Section II. Section III describes the networking scenario and the interference and sensing models and Section IV gives the WLAN channel activity model. In Section V we describe the proposed protocol stack, followed by its mathematical analysis in Section VI. In Section VII we present a numerical evaluation of COG-MAC along with a comparison with traditional WSN MAC schemes, while a simulation study is presented in Section VIII. We concludethe paper in Section IX.

II. RELATED WORK

Energy efficient communications have been extensively studied for stand alone WSNs [3][4]. The key idea for energy efficiency in sensor networks is to minimize idle listening, by letting the sensors turn off their radios whenever idle, controlled by duty-cycling [5][6][8][9], or by wake-up radios [10].

It is recognized, however, that cross-network interference can have significant effect on the network performance, as it is shown for coexisting WSNs in [11] and for WLAN and Bluetooth interference in [12][13].WSN multi-channel operation aims at avoiding this cross-network interferenceby tuning to the best available band for communication [14][15][16].These solutions are efficient as long as there existchannels with no or low interference, but lose effectiveness when all considered channels suffer from interference with similar statistical behavior.

Therefore, as wireless channels are getting densely populated, it is important to design protocols that can work efficiently even in the presence of cross-network interference. Many of the proposed solutions build on the known characteristics of the interfering networks. [17] employs narrowband sensing, with additional HW cost, to identify and utilize the channels, where the wide-band device can effectively coexist with narrow-band transmissions, while in [18], the sensors force the WLAN to back off by sending frequent (one per DIFS), high power jamming signals during their packet transmission, which needs complex PHY layer and leads to increased energy consumption in the WSN. Instead, the effect of interference is minimized without changing the WLAN behavior in [19] and [20] introducing WSN packet header and payload redundancy.

Recent works investigate how to avoid WLAN interferenceby employing channel availability predictions. The case of a non-saturated single WLAN AP is studied in [21], modeling the packet arrivals at the users as a Bernoulli process. In [22] a Poisson arrival process is considered, and WLAN output buffers are modeled as M/G/1 queues, resulting in subgeometric idle period distribution. While these models capture the effect of the WLAN MAC, their generality is limited, since they are based on simple, rather unrealistic traffic models.

To capture the effect of realistic network load, [2][23][24][25] use traffic traces to find the distribution of WLAN idle periods. These results show that idle periods can be short contention periods, in the range of hundreds of microseconds, or heavy-tailed white spaces, where WLAN users are inactive. As it is demonstrated in [25], the average white space length depends on the WLAN load and the traffic characteristics, and is in the milliseconds range. In [26] similar results are derived based on the self-similar nature of WLAN traffic.

Considering that, due to the low bitrate, the transmissiontimes in the WSN are comparable to the average WLAN idle period length, it is important to capture and utilize the heavy tail characteristics of theWLAN channel usage. Therefore, in our work we apply the model of [2][27] where a mixture distribution is proposed to model the idle periods, capturing the two basic sources of inactivity, the long heavy-tailed white space periods, when the WLAN users are inactive, and the short contention windows. Given this WLAN channel usage model we claim that the WSN on one hand needs to avoid channel access in the contention windows and on the otherhand it needs to optimize transmissions in the long whitespace periods [28], which are the key functions in the proposed COG-MAC.

III. NETWORKING SCENARIO, INTERFERENCE AND SENSING MODELS

We consider a WLAN Access Point (AP) zone that covers an area where a WSN is deployed. The WSN

ISSN 2394-3777 (Print)
ISSN 2394-3785 (Online)
Available online at www.ijartet.com
International Journal of Advanced Research Trends in Engineering and Technology (IJARTET)
Vol. 3, Special Issue 24, April 2016

nodes are battery-powered and operate on a single 5MHz channel inside the 2.4GHz ISM band. They transmit information over multiple hops, and are able to estimate the distance to their neighboring nodes [29].

WLAN users are distributed inside the AP zone and operateon a 802.11 22MHz channel, covering the WSN channel. The WLAN transmission power is in the order of 15-20dBm. The WLAN terminals are blind to the WSN nodes [26], that is, the WLAN carrier-sense mechanism does not detect the lowpowerWSN signals, which results in collisions, and hence packet losses in the WSN. On the opposite side, the WSN nodes transmit with a signal power that is in the order of 0-3dBm [30] and, thus, their impact on WLAN operation is negligible [23]. Therefore, to ensure efficient WSN communication, sensor nodes need to consider the WLAN activity when transmitting. In the remainder of this section we clarify

our assumptions on the interference and sensing models used throughout the paper. The signal propagation is assumed to be adequately described by a simple path-loss model. In order to correctly receive a packet, a WSN node needs to receive it with Signal to Interference plus Noise Ratio (SINR) above a given threshold, denoted as _SINR, where the interference is

assumed to be caused by a single active WLAN transmitter. Then, the path loss-based propagation model results in circular interference zones around receiving sensors, with radius RI [31]:

$$R_I(r, \zeta_{\text{SINR}}, \eta, P_{\text{WSN}}, P_{\text{WLAN}}) = \sqrt[\eta]{\frac{\zeta_{\text{SINR}} P_{\text{WLAN}} P_{L_0}}{P_{\text{WSN}} P_{L_0} r^{-\eta} - \zeta_{\text{SINR}} \sigma_N^2}}, \quad (1)$$

where r is the distance between the transmitting and receiving sensor, is the channel path-loss exponent, PWSN is the WSN transmission power, PWLAN is the fraction of WLAN transmission power inside the narrow WSN band, and PL0 and _2N denote the attenuation at 1m reference distance and the noise power, respectively. Whenever an overlap occurs between a WSN packet transmission and a WLAN transmission withinthe receiving sensor node interference zone of radius RI ,weassume that the WSN packet is lost.

The WSN nodes perform channel sensing based on energy detection through their build-in Receiver Signal Strength Indicator (RSSI) [30]. In the proposed system two kinds of sensing are performed. Repeated sensing over long periodsof time for WLAN activity model estimation, and shorttimesensing for channel access control. The performance of both kinds of sensing is bounded by the maximum sensitivity level 0 of the sensor, stating the minimum signal level that can be detected [30]. Short sensing time leads to probabilistic energy detection, characterized by the probability of missed detection, pMD, when a signal is not detected, and the probability of false alarm, pFA, when the sensing results in “signal detected” decision, even when the channel is idle [32]. The false alarm probability pFA is a function of the sensing time ts and of the energy decision threshold, pFA(ts;)=Q((□ _2N)=(_2Np2=(fsts))), where fs denotes the sampling frequency. In this paper we consider a target pFA which gives as [32]:

$$\gamma(p_{\text{FA}}) = \max\left\{\psi_0, \sigma_N^2\left[1 + \sqrt{2/(f_s t_s)}\mathcal{Q}^{-1}(p_{\text{FA}})\right]\right\}. \quad (2)$$

The missed detection probability, pMD, depends on the received signal power, PRx(d), given as a function of the distance to the transmitter d.It also depends on the decision threshold, which in turn is determined, using (2), by the target pFA:

$$p_{\text{MD}}(t_s, d; \gamma(p_{\text{FA}})) = 1 - \mathcal{Q}\left(\frac{\gamma(p_{\text{FA}}) - (\sigma_N^2 + P_{Rx}(d))}{\sigma_N^2\sqrt{2/(f_s t_s)}}\right). \quad (3)$$

During the long-period sensing the sensors keep measuring thechannel to collect samples of active and idle period durations. Due to the longer sensing time, pFA approaches zero. The missed detection probability pMD also approaches zero inside the sensors ACCA, the CCA area, where all transmissions are detected, and approaches 1 outside the ACCA.

Under the path-loss propagation model the CCA area is circular; its radius depends on the WLAN transmission power and can be controlled by tuning the CCA threshold[30]:

$$R_{\text{CCA}} \triangleq R_{\text{CCA}}(\psi) = \left[(\psi - \sigma_N^2)/(P_{\text{WLAN}} P_{L_0})\right]^{-1/\eta}. \quad (4)$$

We derive the COG-MAC performance model consideringpath-loss-based channel attenuation. However, the model can be extended for more generic signal attenuation models, at the expense of increased analytic complexity. In [33] we give the extended model, based on channel attenuation enhanced with

log-normal shadowing, and evaluate the effect of shadowing on the protocol performance in Section VII.

IV. THE WLAN CHANNEL ACTIVITY MODEL

ISSN 2394-3777 (Print)
ISSN 2394-3785 (Online)
Available online at www.ijartet.com
International Journal of Advanced Research Trends in Engineering and Technology (IJARTET)
Vol. 3, Special Issue 24, April 2016

We model the WLAN channel activity as a semi-Markovian system of active and idle periods as originally proposed in [23] and validated in [25]. We call this model the Global View, since it captures the global WLAN activity. Fig. 1(a) depicts the states of the Global View model and their merging into a two-state semi-Markovian chain. The states of Data, SIFS
and ACK transmissions are grouped together into a single Active state and the states that represent the WLAN Contention Window period (CW) and the WLAN white space (WS) due to user inactivity are merged into a single Idle state. The distributions of the active and idle states, fA(t) and fI (t), respectively, define how long the WLAN channel remains in either state. As proposed in [23], a uniform distribution

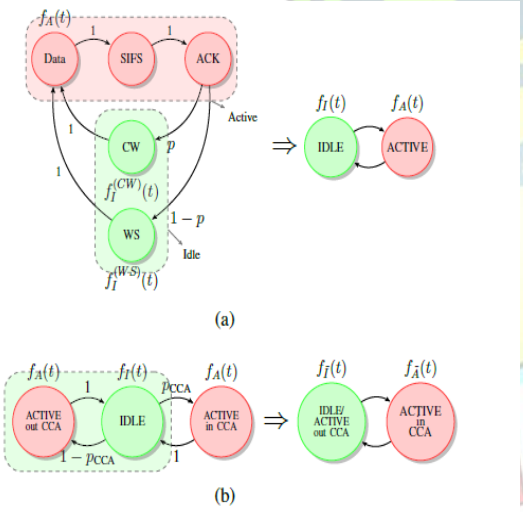

Fig. 1. (a): The Global View model with all channel states and the reduced two-state semi-Markovian model. (b): The 3-state semi-Markovian model and its 2-state equivalent for the Local View channel usage modeling.

in a range [_ON; _ON] sufficiently models the active channel periods. The idle distribution is modeled as a mixture of uniformly distributed idle periods within [0;BK], corresponding to the WLAN contention periods, and long, zero-location generalized Pareto-distributed idle periods with parameters that capture the heavy-tailed behavior of the white spaces. The percentage of contention periods p 2 (0; 1) determines the shape of the mixed idle distribution, which obtains the following form [23]:

$$f_I(t) \triangleq p f_I^{(CW)}(t) + (1-p) f_I^{(WS)}(t) = \begin{cases} p \cdot \frac{1}{\alpha_{BK}} + (1-p) \cdot \frac{1}{\sigma}\left(1+\xi\frac{t}{\sigma}\right)^{-\frac{1+\xi}{\xi}}, & t \le a_{BK}, \\ (1-p) \cdot \frac{1}{\sigma}\left(1+\xi\frac{t}{\sigma}\right)^{-\frac{1+\xi}{\xi}}, & t > a_{BK}, \end{cases} \quad (5)$$

while the active distribution is given as:

$$f_A(t) = 1/(\beta_{ON} - \alpha_{ON}), \quad t \in (\alpha_{ON}, \beta_{ON}). \quad (6)$$

We define the WLAN load as the percentage of time thechannel is active due to WLAN operation:

$$\rho \triangleq \frac{E[T_{ON}]}{E[T_{ON}] + E[T_{OFF}]} = \frac{\frac{\alpha_{ON}+\beta_{ON}}{2}}{p\frac{\alpha_{BK}}{2} + (1-p)\frac{\sigma}{1-\xi}}. \quad (7)$$

Additionally, this provides the probabilities of active and idlechannel at an arbitrary point in time, pA and pI, respectively. Our objective is that of estimating the parameters of the model by means of sensor node observations. Christo Ananth et al. [7] discussed about a method, Wireless sensor networks utilize large numbers of wireless sensor nodes to collect information from their sensing terrain. Wireless sensor nodes are battery-powered devices. Energy saving is always crucial to the lifetime of a wireless sensor network. Recently, many algorithms are proposed to tackle the energy saving problem in wireless sensor networks. There are strong needs to develop wireless sensor networks algorithms with optimization priorities biased to aspects besides energy saving. In this project, a delay-aware data collection network structure for wireless sensor networks is proposed based on Multi hop Cluster Network. The objective of the proposed network structure is to determine delays in the data collection processes. The path with minimized delay through which the data can be transmitted from source to destination is also determined. AODV protocol is used to route the data packets from the source to destination.

It holds that fA~(t) = fA(t), but f~I (t) 6= fI (t); 8pCCA < 1. The observable idle channel
Period consists of a random number of WLAN cycles, that is, consecutive idle and un-detected active periods, followed by an additional idle period. Its distribution, f~I (t), is, therefore, a random-term convolution-based function of the idle and active time distributions, fI (t) and fA(t), and of the observable load pCCA, and can be expressed in closed form only in the Laplace transform (LT) domain, as shown in [34]:

$$f_{\tilde{I}}^*(s) = f_I^*(s) \cdot p_{CCA} \,/\, [1 - (1 - p_{CCA}) f_I^*(s) f_A^*(s)], \quad (8)$$

where f_(s) denotes the Laplace transform of function f.We discuss the feasibility of parameter estimation

ISSN 2394-3777 (Print)
ISSN 2394-3785 (Online)
Available online at www.ijartet.com
International Journal of Advanced Research Trends in Engineering and Technology (IJARTET)
Vol. 3, Special Issue 24, April 2016

in [34][35], where we propose an estimation algorithm that integrates dynamically the collected samples, and therefore runs efficiently on memory-constrained sensor devices.

V. THE COGNITIVE WSN

We propose a WSN COGnitive Medium Access Control (COG-MAC) that employs WLAN usage prediction and channel sensing so as to minimize the energy cost for unicast WSN communication under WLAN interference. In particular, it aims at minimizing the transmission energy spent by sensors for transmitting and receiving data packets. COG-MAC can be combined with some duty-cycling or wake-up enabled solution that is responsible for minimizing the energy spent due to idle listening. Therefore, the COG-MAC design does not consider the idle listening energy costs.

The operation of COG-MAC is divided into two mainphases. The first one is the estimation and optimization phase, when a sensor listens to the channel and gathers samples of the active and idle times, estimates the Local View parameters and selects the optimal one-hop transmission distance and the optimal packet size. The second one is the transmission phase, when the sensor transmits and receives data packets. The sensor moves back to the first phase either periodically, or when it experiences a performance drop, suggesting that the estimated WLAN activity parameters are no longer valid (i.e., WLAN activity has significantly changed).

A. Estimation and optimization

During the estimation phase potential transmitter (TR) and receiver (RR) sensors listen to the channel and gather active and idle times for estimating the WLAN channel activity. As shown in Fig. 2, they perform the measurements for the maximized CCA area ACCA (denoted by AT CCA and AR CCA for TR and RR respectively) by using the maximum sensitivity level 0, leading to RCCA = RCCA(0). Based on these measurements they derive the Local View parameters, that is, the parameters of the functions fA(t); fI (t), and pCCA. The required number of the samples and thus the length of theestimation phase depends on the target estimation accuracy,which in turn is determined by the sensitivity of COG-MAC.Therefore, we discuss this issue in Section VII.

In addition, for a better estimate of the spatial distributionof the active WLAN users, each sensor also evaluates pT CCA, the common load it can observe within the overlap of the CCA areas.Specifically, it measures the load in the disk area A^T

CCA by filtering the measurements with a changed sensitivity level, such that for a TR–RR distance r, ^RCCA =RCCAr. At the end of the estimation phase the sensors receive the observable load values from the potential receivers, denoted by pR CCA.

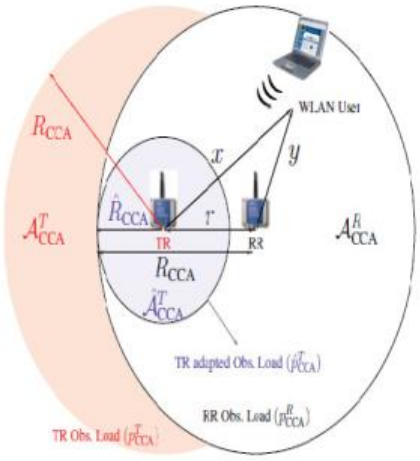

Fig. 2. TR and RR CCA areas, $\mathcal{A}^T_{CCA}$ and $\mathcal{A}^R_{CCA}$, and the adapted CCA area $\hat{\mathcal{A}}^T_{CCA}$.

Based on the locally estimated and received WLAN channel activity model parameters, the sensors select the transmission parameters that are expected to result in minimum energy consumption per bit and meter, according to the model and the implementation given in Section VI. Specifically, they optimize the packet size, to trade-off the probability of interference with a new WLAN transmission and the useful information transmitted per packet. They optimize the transmission distance, to trade-off the probability that a new WLAN transmission does not cause harmful interference and WSN packet transmission can continue even after the white space period, and the progression towards the multihop destination.

B. Transmissions with COG-MAC

The estimation and optimization phase is followed by the transmission phase when actual network operation occurs. We assume that the WSN operates under a duty-cycling or wakeup radio based protocol, to limit the energy that is spent in idle listening [5][10]. In case of duty-cycling, the WSN nodes are synchronized. Synchronization gaps are, however,

ISSN 2394-3777 (Print)
ISSN 2394-3785 (Online)
Available online at www.ijartet.com
International Journal of Advanced Research Trends in Engineering and Technology (IJARTET)
Vol. 3, Special Issue 24, April 2016

expected, as a result of CPU clock drift, and have to be

accounted for. Their maximum value tmax SYNC is determined by the frequency of synchronization dataexchange.Fig. 3 shows the COG-MAC operation within a duty-cycle for potential transmitters (TR) and receivers (RR). The duty cycle of the TR nodes starts with a guard time (denoted as SYNC in the Figure) equal to tmax SYNC, ensuring that channel sensing and transmission do not overlap due to the lack of perfect synchronization. The medium access control is a modified CSMA/CA with the key component of dual channel sensing. As it is shown in Fig. 3, the on time of the duty cycle begins with two short channel sensing measurements

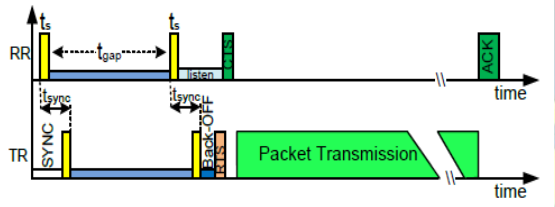

Fig. 3. Time diagram of COG-MAC operations.

with a duration of ts, separated by a time gap of tgap, whereON tgap BK. The sensor's RF circuit can be powered-off between the short channel measurements. If the channel state is correctly detected as idle at both measurements, the sensors can safely assume that the spectrum was idle in the entire time and characterize the idle period as a white space. The operation in the rest of the cycle is determined by the sensing result. If any of the measurements have indicated an active state, the sensor immediately transits to sleep mode to save energy. Instead, sensors with idle measurements stay awake and follow a CSMA/CA-based channel access with RTS/CTS exchange. RTS/CTS has been shown to be beneficial in [28], as it allows TR and RR to share their view on the channel status, and increases the probability that the current period is indeed a long white-space (and not the case when a WLAN station is transmitting outside the CCA area), as the total observable load includes the percentage seen by the RR node. We evaluate the usefulness of RTS/CTS under fixed packet size in Section VII. Sensors are assumed to transit to sleep mode after packet transmission, and retransmit packets, if required, in consecutive duty cycle periods.

VI. COG-MAC OPTIMIZATION

In this Section we define the COG-MAC energy consumption model, and formulate the packet size and transmission distance optimization problem. This formulation allows us to trade-off the probability of successful packet transmission with its usefulness, considering the amount of informationtransmitted and the distance travelled. Then we present thedetailed analytic model of COG-MAC that is required for the optimization. Due to space limitation the presentation is restricted to the case of perfect synchronization, RTS/CTS-based access and simple path-loss model. Interested readers can find the respective model extensions in [28][33]. Moreover, in order to focus on the effect of WLAN interference, we consider the case of low WSN load, when the probability of sensors competing for the channel is low. The model can be extended for the high load case, including expected delays of channel access due to contention resolution.

A. Energy efficiency optimization

COG-MAC consumes energy for computing and storing the optimal transmission parameters, for packet transmission, and for sensing, listening and packet reception. Below we focus on the energy spent for radio operations, as their energy consumption in typical sensor nodes is at least two orders of magnitude higher than that of computations. We consider the WSN communication to be energy optimal when the energy cost of transmitting and receiving a unit of information at unit distance is minimized. Therefore, we define the main performance measure as the energy consumption at the TR and RR nodes until successful packet delivery, that is, through the sequence of possibly unsuccessful and eventually successful RTS/CTS handshake and packet transmission attempts, normalized by the amount of information transmitted and the distance covered.

We consider a fixed power cost, PWSN ON, for channel sensing, transmitting, receiving, and idle listening during the RTS/CTS handshake. Consequently, the expected TR energy cost of attempting a handshake is eTRhs = PWSN ON (ths + 2ts), where, ths are, respectively, the durations of the repeated sensing and the handshake. The latter includes the synchronization gap and the RTS/CTS process. Let T denote the event of successful handshake. Assuming that the WLAN channel state is uncorrelated at the consecutive handshake attempts, the number of unsuccessful handshakes has geometric distribution with parameter PfT g, and the expected energy cost until handshake success becomes:

$$E_{\mathrm{hs}}^{\mathrm{TR}}(r) = e_{\mathrm{hs}}^{\mathrm{TR}} / P\{\mathcal{T}\}. \qquad (9)$$

ISSN 2394-3777 (Print)
ISSN 2394-3785 (Online)
Available online at www.ijartet.com
International Journal of Advanced Research Trends in Engineering and Technology (IJARTET)
Vol. 3, Special Issue 24, April 2016

At the receiver, the handshake energy cost, eRRhs , depends on whether the node has participated in the handshake. Under perfect synchronization and considering ths >> ts the expected cost can be approximated as:

$$e_{\text{hs}}^{\text{RR}} \approx \begin{cases} e_{\text{hs}}^{\text{TR}}, & \text{RR participates in HS} \\ 0, & \text{otherwise.} \end{cases} \quad (10)$$

Similar to (9), the expected handshake cost will be:

$$E_{\text{hs}}^{\text{RR}}(r) = e_{\text{hs}}^{\text{TR}} \left[1 + (1/P\{\mathcal{T}\} - 1) \cdot P\{\mathcal{T}_P|\overline{\mathcal{T}}\}\right], \quad (11)$$

with PfTP jT g denoting the probability that RR has participatedon an, otherwise, failed handshake attempt. The energy cost for transmitting and for receiving a packet with transmission time t is, similarly, PWSN ON t. If a packet transmission attempt fails, a new handshake must be established before attempting a new transmission. Consequently, the expected energy cost of successful packet delivery with packet transmission time t becomes:

$$E_{\text{trans}}(r,t) = 1/P\{\text{transmission success}|\mathcal{T}\} \cdot \cdot\left[E_{\text{hs}}^{\text{TR}}(r) + E_{\text{hs}}^{\text{RR}}(r) + 2 \cdot P_{\text{ON}}^{\text{WSN}} \cdot t\right]. \quad (12)$$

$$(t^*, r^*) = \arg\min_{t,r} \{E_{\text{trans}}(r,t)\,[r \cdot (R_{\text{WSN}} t - L_0)]\}, \quad (13)$$

where RWSN and L0 denote the WSN transmission rate andthe packet overhead, respectively. (13) can be easily modified to consider only t or r WSNs with known node distance or packet size respectively.
We derive the optimal values numerically by solving theabove optimization problems applying the bisection method. For practical implementation the optimization problem can be solved a-priori, and the optimal packet size and next-hop distance pairs for a set of WLAN load parameter vectors can be stored in the sensor.

B. COG-MAC probability of successful handshake and transmission

In this Section we derive analytically the probabilities of successful handshake and packet transmission, required in (9),(12), respectively. The TR starts a handshake by transmitting an RTS packet, if its dual sensing process gave idle channel status. Let
the events that the i-th channel measurement is idle at the TR and RR nodes, respectively, with i = 1; 2. The Handshake attempt is successful if the RR node is awake, as a result of a pair of idle measurements, and, additionally, if the communication is not disturbed by an ongoing, miss-detected WLAN transmission, or by a WLAN transmission that starts during the period of the handshake within the TR or RR interference regions. After a successful handshake the packet transmission itself will be successful, if all WLAN sources within the interference region of the RR remain silent during the whole packet transmission time. We derive the probability of successful handshake and transmission in five steps.
1) We define the spatial distribution of WLAN sources, as seen by the TR node, based on the a priori measured observable load values and the TR-RR distance r.
2) Using Bayesian inference we derive the probability of idle and active channel status at the TR and RR nodes, given the observed idle state measurements at the TR.
3) We derive the distribution of the interference-free time that remains after the dual sensing process.
4) Based on the previous steps, we express the probability of a successful handshake between the TR and the RR node.
5) Finally, conditioned on the successful handshake, the probability of successful packet transmission success g is expressed as a function of transmission distance and packet length. Let S 2 S = fIg [fAXY(x; y) : x 2 X; y 2 Yg be the channel status. The status is either idle, I, or active, AXY(x; y), with a WLAN source at distances (X; Y) = (x; y) 2 X _Y from the TR and RR nodes, respectively (see Fig. 2). X _ Y denotes the set of all possible WLAN source positions.
S(i) 2 S denotes the channel status during the i-th sensing measurement, where i = 1; 2.
1) Spatial distribution of WLAN interfering sources: The spatial distribution of WLAN sources around the TR and RR nodes affects their miss-detection probabilities, as well as the probability that such a source within the TR/RR interference region starts to transmit during the WSN packet transmission.
As shown in Fig. 2, the TR can estimate the joint distribution of the distances X,Y of a possible active WLAN source based on the a-priori known observable load values, pR CCA, received from RR, and ^pT CCA, measured by the TR itself. Since A^T CCA _ AR CCA, an arbitrary WLAN source lies in the area A^T CCA with probability ^pT CCA, in the area AR CCA n A^T CCA with probability pR CCA ^pT CCA, and in the AP area outside AR CCA otherwise. Since there is no additional a-priori information available about the WLAN source locations, the TR assumes that these sources are located uniformly at random inside the respective areas. In addition, we approximate the AP area as a disc around TR with radius Rmax. This approximation does not affect the model accuracy significantly, unless the TR happens to be very close

ISSN 2394-3777 (Print)
ISSN 2394-3785 (Online)
Available online at www.ijartet.com
International Journal of Advanced Research Trends in Engineering and Technology (IJARTET)
Vol. 3, Special Issue 24, April 2016

to the border of the AP area. Let fX(x) denote the unconditional probability density function of distance X, for uniformly random WLAN source locations in an disk area around TR with radius Rmax. Similarly, fY jX(x; y) denotes the density of the distance Y from the RR node, given X=x, and fXY (x; y) = fX(x)fY jX(x; y) denotes the unconditional joint distance density.

$$p_{A_X}(x)=f_X(x)\cdot\begin{cases}\hat{p}^T_{\mathrm{CCA}}\,/\,\nu_{\hat{R}_{\mathrm{CCA}}}, & x\le\hat{R}_{\mathrm{CCA}},\\ \frac{F_{Y|X}(x,R_{\mathrm{CCA}})(p^R_{\mathrm{CCA}}-\hat{p}^T_{\mathrm{CCA}})}{\nu_{R_{\mathrm{CCA}}}-\nu_{\hat{R}_{\mathrm{CCA}}}}+ & \\ +\frac{\overline{F}_{Y|X}(x,R_{\mathrm{CCA}})(1-p^R_{\mathrm{CCA}})}{1-\nu_{R_{\mathrm{CCA}}}}, & \text{other.},\end{cases} \tag{14}$$

whereRCCA denote the ratio of the observable areas A^T CCA and AR CCA, respectively, over the total WLAN AP area with radius Rmax. Similarly, the conditional distance density pAY jX(x; y), can be expressed as:

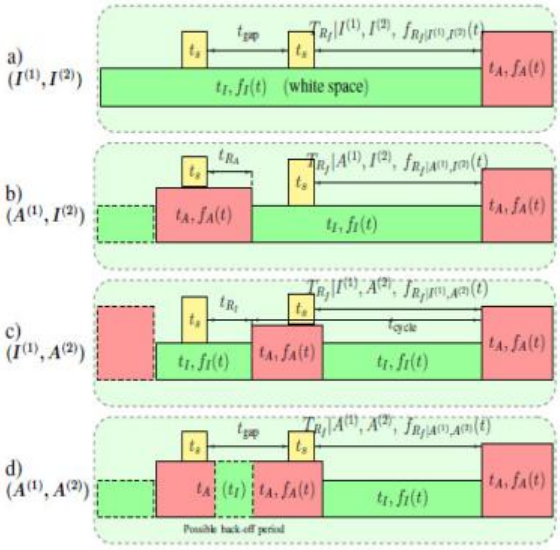

Fig. 4. Diagram for the calculation of remaining time densities.

$$p_{A_{Y|X}}(x,y)=$$
$$f_{Y|X}(x,y)\cdot\begin{cases}\hat{p}^T_{\mathrm{CCA}}\,/\,\nu_{\hat{R}_{\mathrm{CCA}}}, & x\le\hat{R}_{\mathrm{CCA}}\\ \frac{p^R_{\mathrm{CCA}}-\hat{p}^T_{\mathrm{CCA}}}{\nu_{R_{\mathrm{CCA}}}-\nu_{\hat{R}_{\mathrm{CCA}}}}, & x>\hat{R}_{\mathrm{CCA}}, y\le R_{\mathrm{CCA}}\\ \left(1-p^R_{\mathrm{CCA}}\right)/\left(1-\nu_{R_{\mathrm{CCA}}}\right), & \text{otherwise.}\end{cases} \tag{15}$$

2) Bayesian inference of channel status: We derive now the posterior distribution of channel status, S(1); S(2) given the observed TR idle measurements, applying Bayesian formulation. To calculate Pf S(1); S(2)T g we use the following decomposition:

$$\begin{aligned}&P\{(S^{(1)},S^{(2)})\,|\hat{I}^{(1)}_T,\hat{I}^{(2)}_T\}=\\ &=P\{S^{(1)}|\hat{I}^{(1)}_T,\hat{I}^{(2)}_T\}\cdot P\{S^{(2)}|S^{(1)},\hat{I}^{(1)}_T,\hat{I}^{(2)}_T\}=\\ &=P\{S^{(1)}|\hat{I}^{(1)}_T\}\cdot P\{S^{(2)}|S^{(1)},\hat{I}^{(2)}_T\}.\end{aligned} \tag{16}$$

$$P\{I^{(1)}|\hat{I}^{(1)}_T\}=\frac{(1-p_{\mathrm{FA}})p_I}{\int_{\mathcal{X}}p_{\mathrm{MD}}(u)p_{A^{(1)}_X}(u)du+(1-p_{\mathrm{FA}})p_I}, \tag{17}$$

$$P\{A^{(1)}_X|\hat{I}^{(1)}_T\}=\frac{p_{\mathrm{MD}}(x)p_{A^{(1)}_X}(x)}{\int_{\mathcal{X}}p_{\mathrm{MD}}(u)p_{A^{(1)}_X}(u)du+(1-p_{\mathrm{FA}})p_I}, \tag{18}$$

$$P\{A^{(1)}_{\mathrm{XY}}|\hat{I}^{(1)}_T\}=\frac{p_{\mathrm{MD}}(x)p_{A^{(1)}_{\mathrm{XY}}}(x,y)}{\iint_{\mathcal{XY}}p_{\mathrm{MD}}(u)p_{A^{(1)}_{\mathrm{XY}}}(u,v)dudv+(1-p_{\mathrm{FA}})p_I} \tag{19}$$

Conditioned on the first idle measurement the channel statusis either idle or active with the following probabilities: where pA(1) X (x) = pA_pAX(x) is the probability that a WLAN source is active at a distance x from the TR at the time of the first measurement, and pA(1) XY (x; y) = pA _ pAXY (x; y) is the probability that it is active at distances x; y from TR and RR respectively. To derive the second term of (16), we first express the status transition probabilities, PfS(2)jS(1)g, following Fig. 4. For I(1) (Fig. 4(a),(c)):

$$P\{I^{(2)}|I^{(1)}\}=\overline{F}_{R_I}(t_{\mathrm{gap}}), \tag{20}$$

$$P\{A^{(2)}_{\mathrm{XY}}|I^{(1)}\}=\left(1-P\{I^{(2)}|I^{(1)}\}\right)p_{A_{\mathrm{XY}}}(x,y). \tag{21}$$

In the above, FRI (t) denotes the distribution function of theremaining idle time, TRI , As the time of the first measurement is uniformly distributed within the WLAN idle period: FRI (t) = R1 t (1 t z)fI (z)dz. Similarly, for S(1) = A(1) XY; 8x; y we obtain (Fig. 4(b)):

$$P\{I^{(2)}|A^{(1)}_{\mathrm{XY}}\}=\int_0^{t_{\mathrm{gap}}}\overline{F}_I(t_{\mathrm{gap}}-z)f_{R_A}(z)dz, \tag{22}$$

$$\begin{aligned}&P\{A^{(2)}_{\mathrm{XY}}|A^{(1)}_{\mathrm{XY}}(x_1,y_1)\}=\overline{F}_{R_A}(t_{\mathrm{gap}})\delta(x_1,y_1)+\\ &+[1-\overline{F}_{R_A}(t_{\mathrm{gap}})-P\{I^{(2)}|A^{(1)}_{\mathrm{XY}}\}]p_{A_{\mathrm{XY}}}(x,y).\end{aligned} \tag{23}$$

Finally, we define the channel status probabilities conditioned on the second idle measurement and based on the a-priori status transition probabilities calculated in (20)-(23):

ISSN 2394-3777 (Print)
ISSN 2394-3785 (Online)
Available online at www.ijartet.com
International Journal of Advanced Research Trends in Engineering and Technology (IJARTET)
Vol. 3, Special Issue 24, April 2016

$$P\{I^{(2)}|I^{(1)},\hat{I}_T^{(2)}\} = \\ = \frac{(1-p_{FA})P\{I^{(2)}|I^{(1)}\}}{(1-p_{FA})P\{I^{(2)}|I^{(1)}\}+\int\int_{XY} p_{MD}(u)P\{A_{XY}^{(2)}|I^{(1)}\}dudv},$$

$$P\{A_{XY}^{(2)}|I^{(1)},\hat{I}_T^{(2)}\} = \left(1-P\{I^{(2)}|I^{(1)},\hat{I}_T^{(2)}\}\right)p_{A_{XY}}(x$$

$$P\{I^{(2)}|A_{XY}^{(1)},\hat{I}_T^{(2)}\} = \\ = \frac{(1-p_{FA})P\{I^{(2)}|A_{XY}^{(1)}\}}{(1-p_{FA})P\{I^{(2)}|A_{XY}^{(1)}\}+\int\int_{XY} p_{MD}(u)P\{A_{XY}^{(2)}|A_{XY}^{(1)}\}dudv}$$

$$P\{A_{XY}^{(2)}|A_{XY}^{(1)}(x_1,y_1),\hat{I}_T^{(2)}\} = \\ = \frac{p_{MD}(x)P\{A_{XY}^{(2)}|A_{XY}^{(1)}(x_1,y_1)\}}{(1-p_{FA})P\{I^{(2)}|A_{XY}^{(1)}\}+\int\int_{XY} p_{MD}(u)P\{A_{XY}^{(2)}|A_{XY}^{(1)}\}dudv}$$

3) Conditional remaining interference-free time: We define TRF , T(TR,RR) RF as the total interference-free time remaining at the RR sensor and at both the TR and RR sensors, respectively, after the sensing process at the nodes, and derive the densities fRF jS(1);S(2) (t) and f(TR,RR) RF jS(1);S(2) (t), given the channel status at the time of the TR measurements. TRF includes the interval between the end of the second sensing measurement and the start of the following active WLAN period, and a geometric number of successive WLAN cycles, i.e. pairs of successive active and idle WLAN periods with density fC(t) = fI (t)_fA(t), representing consecutive WLAN
Transmissions outside the interference area. The distribution of TRF can be numerically calculated with the help of Laplace transform, similar to (8) and for all S(1); S(2) 2 S:

$$f_{R_F|S^{(1)},S^{(2)}}(t) = \mathcal{L}^{-1}\left\{\frac{p_{\mathcal{I}\mathcal{N}} f^*_{R_f|S^{(1)},S^{(2)}}(s)}{1-(1-p_{\mathcal{I}\mathcal{N}})f_I^*(s)f_A^*(s)}\right\}, \quad (28)$$

For additionally undisturbed TR, we obtain the density:

$$f^{(TR,RR)}_{R_F|S^{(1)},S^{(2)}}(t) = \mathcal{L}^{-1}\left\{\frac{p^{(TR,RR)}_{\mathcal{I}\mathcal{N}} f^*_{R_f|S^{(1)},S^{(2)}}(s)}{1-(1-p^{(TR,RR)}_{\mathcal{I}\mathcal{N}})f_I^*(s)f_A^*(s)}\right\}, \quad (29)$$

Where pIN, the probability that an activated WLAN source interferes with the RR reception is:

$$p_{\mathcal{I}\mathcal{N}} = \begin{cases} p^R_{CCA}\left(R_{\mathcal{I}}(r)/R_{CCA}\right)^2, \text{ if } R_{\mathcal{I}}(r) \le R_{CCA} \\ p^R_{CCA} + (1-p^R_{CCA})\frac{R^2_{\mathcal{I}}(r)-R^2_{CCA}}{R^2_{max}-R^2_{CCA}}, \text{otherwise,} \end{cases} \quad (30)$$

and the probability that the source lies, additionally, inside the TR interference area is given as:

$$p^{(TR,RR)}_{\mathcal{I}\mathcal{N}} = \int_{y\le R_{\mathcal{I}}(r)}\int_{x\le R_{\mathcal{I}}(r)} p_{A_{XY}}(x,y)dxdy. \quad (31)$$

The interval between the end of the second sensing measurement and the start of the first active WLAN period is denoted by TRf , and its density depends on the channel status. In the derivations we approximate the sensing period as Ts = 2ts + tgap _ tgap, since tgap _ ts.

For I(1); I(2) (Fig. 4(a)) we safely classify the idle period as white space, and consequently.

$$f_{R_f|I^{(1)},I^{(2)}}(t) = f_{R_I}(t+t_{gap})/\overline{F}_{R_I}(t_{gap}). \quad (32)$$

In the case (A(1)XY; I(2)) (Fig. 4(b)), a transition from active to idle status occurs sometime z _ tgap after the first TR measurement, and the idle period may also be a back-off, which gives:

$$f_{R_f|A^{(1)}_{XY},I^{(2)}}(t) = \frac{1}{F_{R_A}(t_{gap})}\int_0^{t_{gap}} f_{R_A}(z)\frac{f_I(t+t_{gap}-z)}{\overline{F}_I(t_{gap}-z)}dz. \quad (33)$$

For S(2) = A(2)XY (Fig. 4(c)) the channel is active at the second measurement, and the remaining time, TRf , is given by the remaining active and the following idle period:

$$f_{R_f|I^{(1)},A^{(2)}_{XY}}(t) = \frac{1}{F_{R_I}(t_{gap})}\int_0^{t_{gap}} f_{R_I}(z)\frac{f_C(t+t_{gap}-z)}{\overline{F}_A(t_{gap}-z)}dz. \quad (34)$$

Finally under (A(1)XY ;A(2) XY) (Fig. 4(d)), the active period may be continuous between the two measurements, or interrupted by a short idle time. In the case of continuous activeperiod:

$$f_{R_f|A^{(1)}_{XY}(x_1,y_1),A^{(2)}_{XY}(x_1,y_1)}(t) = \\ = \frac{1}{\overline{F}_{R_A}(t_{gap})}\int_{t_{gap}}^{\infty} f_{R_A}(z)f_I(t+t_{gap}-z)dz, \quad (35)$$

while in the case of a short idle period between the measurements, (x1; y1) 6= (x2; y2):

$$f_{R_f|A^{(1)}_{XY},A^{(2)}_{XY}}(t) = \frac{1}{\overline{F}_{R_A}(t_{gap})}\cdot \\ \cdot\int_0^{t_{gap}} f_{R_A}(z_1)\frac{\int_0^{t_{gap}-z_1} f_I(z_2)}{F_I(t_{gap}-z_1)}\cdot\frac{f_{cycle}(t+t_{gap}-z_1-z_2)}{\overline{F}_A(t_{gap}-z_1-z_2)}dz_1dz_2. \quad (36)$$

ISSN 2394-3777 (Print)
ISSN 2394-3785 (Online)
Available online at www.ijartet.com
International Journal of Advanced Research Trends in Engineering and Technology (IJARTET)
Vol. 3, Special Issue 24, April 2016

4) TR-RR handshake success: For a TR node aiming at communicating with an RR at distance r we calculate the probability of successful handshake, conditioned on the idle TR measurements. The event of handshake success, requires, first, idle measurements at the receiver, ^I(1)R ; ^I(2)R . Second, it requires that no WLAN transmission interferes with the RTS/CTS handshake. Since the duration of the handshake is expected to be significantly lower than the WLAN activity dynamics, we approximate the second constraint as the requirement that all the active WLAN sources lie outside the interference regions of both the TR and the RR for the entire handshake period:

$$P\{\mathcal{T}|S^{(1)},S^{(2)}\} \approx P\{\hat{I}_R^{(1)},\hat{I}_R^{(2)}|S^{(1)},S^{(2)}\}\overline{F}^{(\mathrm{TR,RR})}_{R_F|S^{(1)},S^{(2)}}(t_{\mathrm{hs}}). \tag{37}$$

If the channel status is indeed idle during both of the TRmeasurements, i.e., (S(1); S(2)) = (I(1); I(2)), the handshake is successful if there is no false alarm at the RR, and the remaining interference-free time at both the RR and TR is longer than the total duration of the handshake ths. That is:

$$P\{\mathcal{T}|I^{(1)},I^{(2)}\} = (1-p_{\mathrm{FA}})^2\overline{F}^{(\mathrm{TR,RR})}_{R_F|I^{(1)},I^{(2)}}(t_{\mathrm{hs}}). \tag{38}$$

With a similar reasoning, the conditional handshake successprobability for the remaining channel status cases becomes:

$$P\{\mathcal{T}|A_{\mathrm{XY}}^{(1)}(x,y),I^{(2)}\} = \\ = (1-p_{\mathrm{FA}})p_{\mathrm{MD}}(y)\overline{F}^{(\mathrm{TR,RR})}_{R_F|A_{\mathrm{XY}}^{(1)},I^{(2)}}(t_{\mathrm{hs}}),\ x\in\mathcal{X},y\in\mathcal{Y}, \tag{39}$$

$$P\{\mathcal{T}|I^{(1)},A_{XY}^{(2)}(x,y)\} = \\ = (1-p_{FA})p_{\mathrm{MD}}(y)\overline{F}^{(\mathrm{TR,RR})}_{R_F|I^{(1)},A_{\mathrm{XY}}^{(2)}}(t_{\mathrm{hs}}),\ x,y\geq R_I(r), \tag{40}$$

$$P\{\mathcal{T}|A_{\mathrm{XY}}^{(1)}(x_1,y_1),A_{\mathrm{XY}}^{(2)}(x_2,y_2)\} = \\ = p_{\mathrm{MD}}(y_1)p_{\mathrm{MD}}(y_2)\overline{F}^{(\mathrm{TR,RR})}_{R_F|A_{\mathrm{XY}}^{(1)},A_{\mathrm{XY}}^{(2)}}(t_{\mathrm{hs}}),x_2,y_2\geq R_I(r). \tag{41}$$

The probability of handshake success is then calculated byaveraging over all possible cases (Eq. (42)). Finally, we calculate the conditional probability PfTP jT g needed in (11) applying Bayesian inference:

$$P\{\mathcal{T}_P|\overline{\mathcal{T}}\} \triangleq P\{\text{RR attempting HS}|\text{HS failed}\} = \\ = 1-P\{\text{RR not attempt. HS}|\text{HS failed}\} = \\ = 1-P\{\text{RR not attempt. HS}\}/\left[1-P\{\mathcal{T}|\hat{I}_T^{(1)},\hat{I}_T^{(2)}\}\right] \tag{43}$$

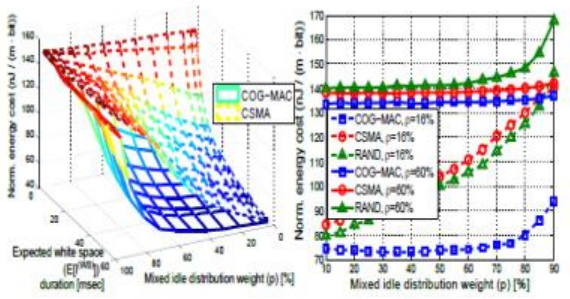

(a) (b)

Fig. 5. (a) Comparison of Cognitive and CSMA-based MAC over p and σ, and (b) normalized energy cost with respect to p for fixed WLAN Load ($\rho = 16\%$ and 60%)

5) Successful packet transmission: Finally, let us expressthe probability of successful packet transmission, now conditioned on the success of the handshake. We update all (S(1); S(2)), through Bayesian inference:

$$P\{S^{(1)},S^{(2)}|\mathcal{T}\} = P\{S^{(1)},S^{(2)}|\mathcal{T},\hat{I}_T^{(1)},\hat{I}_T^{(2)}\} = \\ = \frac{P\{\mathcal{T}|S^{(1)},S^{(2)},\hat{I}_T^{(1)},\hat{I}_T^{(2)}\}P\{S^{(1)}S^{(2)}|\hat{I}_T^{(1)},\hat{I}_T^{(2)}\}}{P\{\mathcal{T}|\hat{I}_T^{(1)},\hat{I}_T^{(2)}\}} = \\ = \frac{P\{\mathcal{T}|S^{(1)},S^{(2)}\}P\{S^{(1)}S^{(2)}|\hat{I}_T^{(1)},\hat{I}_T^{(2)}\}}{P\{\mathcal{T}|\hat{I}_T^{(1)},\hat{I}_T^{(2)}\}}, \tag{44}$$

where PfT j^I(1)T ; ^I(2) T g is defined in (42), the terms PfT jS(1); S(2)g are derived in the previous section and PfS(1); S(2)j^I(1) T ; ^I(2) T g is derived from (16). Similarly, we update the total remaining interference-free time, TRF , with respect to the total length of the handshake time, including the synchronization delay, tThs = ths + tSYNC, as it is measured by the TR node:

$$\overline{F}_{R_F|(S^{(1)},S^{(2)}),\mathcal{T}}(t) = \\ = P\{T_{R_F}\geq t+t_{\mathrm{hs}}^T|T_{R_F}^{(\mathrm{TR,RR})}\geq t_{\mathrm{hs}}^T\} = \\ = \frac{P\{T_{R_F}\geq t+t_{\mathrm{hs}}^T,T_{R_F}^{(\mathrm{TR,RR})}\geq t_{\mathrm{hs}}^T\}}{P\{T_{R_F}^{(\mathrm{TR,RR})}\geq t_{\mathrm{hs}}^T\}} \approx \frac{\overline{F}_{R_F|(S^{(1)},S^{(2)})}(t+t_{\mathrm{hs}}^T)}{\overline{F}^{(\mathrm{TR,RR})}_{R_F|(S^{(1)},S^{(2)})}(t_{\mathrm{hs}}^T)}, \tag{45}$$

where the respective density functions are given in (28) and(29), and the approximation is valid due to the relatively short WSN handshake time with respect to the average WLAN cycle duration. Finally, from (42) and (45) we express the probability that a packet of transmission duration t will be successfully transmitted as:

$$P\{\text{transmission success}|\mathcal{T}\} = \\ = \sum\overline{F}_{R_F|(S^{(1)},S^{(2)}),\mathcal{T}}(t)P\{S^{(1)},S^{(2)}|\mathcal{T},\hat{I}_T^{(1)},\hat{I}_T^{(2)}\}, \tag{46}$$

ISSN 2394-3777 (Print)
ISSN 2394-3785 (Online)
Available online at www.ijartet.com
International Journal of Advanced Research Trends in Engineering and Technology (IJARTET)
Vol. 3, Special Issue 24, April 2016

$$P\{\mathcal{T}|\hat{I}_T^{(1)},\hat{I}_T^{(2)}\} = P\{\mathcal{T}|I^{(1)},I^{(2)}\}P\{I^{(1)},I^{(2)}|\hat{I}_T^{(1)},\hat{I}_T^{(2)}\} + \iint_{\mathcal{XY}} P\{\mathcal{T}|A_{\mathrm{XY}}^{(1)}(x,y),I^{(2)}\}P\{A_{\mathrm{XY}}^{(1)}(x,y),I^{(2)}|\hat{I}_T^{(1)},\hat{I}_T^{(2)}\}dxdy$$
$$+ \iint_{x,y\geq R_I(r)} P\{\mathcal{T}|I^{(1)},A_{\mathrm{XY}}^{(2)}(x,y)\}P\{I^{(1)},A_{\mathrm{XY}}^{(2)}(x,y)|\hat{I}_T^{(1)},\hat{I}_T^{(2)}\}dxdy \quad (42)$$
$$+ \iint_{\mathcal{XY}}\iint_{x_2,y_2\geq R_I(r)} P\{\mathcal{T}|A_{\mathrm{XY}}^{(1)}(x_1,y_1),A_{\mathrm{XY}}^{(2)}(x_2,y_2)\}P\{A_{\mathrm{XY}}^{(1)}(x_1,y_1),A_{\mathrm{XY}}^{(2)}(x_2,y_2)|\hat{I}_T^{(1)},\hat{I}_T^{(2)}\}dx_1dy_1dx_2dy_2.$$

where the summation is over all possible channel statusS(1); S(2).

VII. NUMERICAL PERFORMANCE EVALUATION

We evaluate the performance of COG-MAC, based on the analytic model in Section VI, by comparing it to noncognitive WSN MAC schemes that – similar to COG-MAC – are controlled by duty-cycling. In particular, we consider an ALOHA-type Random Access MAC (RAND), where sensors transmit without any channel sensing before transmission, and a standard 802.15.4-compliant carrier-sense (CSMA) MAC scheme, where WSN nodes perform the standard channel

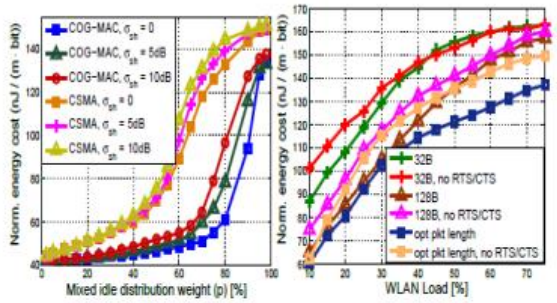

(a) $\bar{T}^{\mathrm{WS}} = 60$ms (b) $p = 0.8$

Fig. 6. (a) COG-MAC – CSMA comparison with respect to the normalized energy cost under log-normal shadowing and (b) fixed packet lengths.

TABLE I
PARAMETER SETUP FOR THE PERFORMANCE EVALUATION

Channel Model	
Path-Loss Exponent (η)	3.0
Ref. Distance attenuation (P_{L_0})	Isotropic $(\lambda/(4\pi)))^2$
Noise Power (σ_N^2)	-174 dB/Hz
WLAN Properties & Modeling	
Bandwidth (B_{WLAN})	22MHz (802.11x Channel)
Tx-Power	18dBm (22MHz Channel)
Tx-Power inside WSN band (P_{WLAN})	12dB
Max. back-off period (α_{BK})	700μsec
Active period interval ($\alpha_{\mathrm{ON}}, \beta_{\mathrm{ON}}$)	(0.8msec, 1.5msec)
White space Pareto scale (ξ)	0.3095
WSN & CC2420 Properties	
Bandwidth (B_{WSN})	5MHz Zigbee Channel
Tx-Power (P_{WSN})	1dBm
Tx-Rate (R_{WSN})	250kbps
Header Length [Packet overhead] (L_0)	13 bytes
RTS/CTS Length	6 bytes
Minimum SINR (ζ_{SIR})	5dB
Receiver Sensitivity (ψ)	-100 dBm
RSSI Dynamic Range	100dB
Tx/Rx Power Consumption ($P_{\mathrm{ON}}^{\mathrm{WSN}}$)	55mW
Handshake Duration (t_{hs})	768μsec
Channel Sensing Model	
Sampling Frequency (f_s)	5MHz
Sensing Time (t_s)	16μsec
False Alarm Constraint (p_{FA})	10^{-2}

Sensing and RTS/CTS handshake. The analytic models forCSMA and RAND are similar to that of COG-MAC and are not presented here due to space limitation. Interested readers can find them in [33], in Sections VII-A, VII-B, respectively. In addition, we evaluate the effect of the channel model on the protocols' performance, by considering lognormal shadowing. Shadowing affects both channel sensing and interference and, therefore, the resulting energy cost. We present the analytic model extensions for COG-MAC and CSMA under log-normal shadowing in Sections VI-C and VIIA of [33], respectively. Finally, to evaluate the importance of the handshake process, we compare COG-MAC performance with and without RTS/CTS mechanism, derived from the model in [28]. For all schemes we consider the normalized energy cost metric under optimized transmission distance and packet size as defined by

ISSN 2394-3777 (Print)
ISSN 2394-3785 (Online)
Available online at www.ijartet.com
International Journal of Advanced Research Trends in Engineering and Technology (IJARTET)
Vol. 3, Special Issue 24, April 2016

(13). The default parameters of our reference evaluation scenario are listed in Table I.

A. Comparison with RAND & CSMA schemes

Fig. 5(a) compares the normalized energy cost of COGMAC and CSMA with respect to the parameter p, the percentage of short WLAN back-off intervals, and E the average length of white spaces, controlled by the shape parameter _ of the generalized Pareto distribution. We set the observable load at the receiving sensor at pR CCA = 0:5. To consider random transmitter location we randomize ^pT CCA, following a normalized binomial distribution, in [0; pRCCA]. In general, increasing p or decreasing E increases the load and consequently the normalized energy consumption for both protocols. Fig. 5(a), however, shows that COGMAC significantly outperforms CSMA. In Fig. 5(b) we keep the load constant at _ = 16% and 60%, and increase the percentage of the back-off periods p. Even in this case COGMAC shows better normalized energy consumption compared to both CSMA and RAND. The energy cost of COG-MAC is only marginally affected by the growing percentage of back off periods. In contrast, RAND and CSMA, due to the fact

that they have to optimize transmission parameters for the mixture idle time distribution, cannot provide energy efficient communication for a large range of p. Under high percentage of back-off idle periods RAND exhibits a performance drop due to the absence of the RTS/CTS mechanism, as failed transmission attempts result in a high energy cost at the receiving nodes. On the contrary, handshake-enabled protocols are more energy efficient due to a lower rate of packet transmission failures.

1) Impact of channel shadowing: Fig. 6(a) compares COG-MAC to CSMA under log-normal shadowing channel model and for various shadowing standard deviation (_sh) values. Shadowing on the wireless channel degrades the WSN communication energy efficiency as it adds uncertainty in both the WLAN spatio-temporal model estimation and the interference calculation, and the degradation is significant for COG-MAC at high WLAN load. Still, the large performance gap between the two solutions remains.

2) Impact of the RTS/CTS handshake mechanism: Fig. 6(b)compares the efficiency of COG-MAC with and without RTS/CTS exchange under increasing WLAN channel load decreasing average white-spacesduration – and for fixed andoptimized WSN packet lengths. We observe that RTS/CTS is always beneficial under optimized packet lengths. As discussed in Section VII-A the absence of the handshake mechanism degrades the energy efficiency under high channel

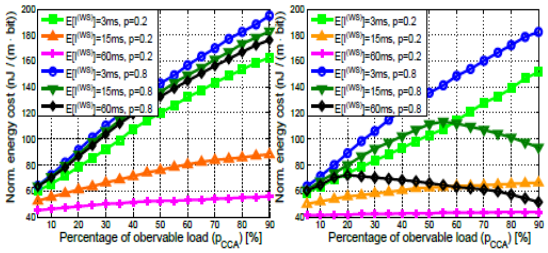

(a) CSMA (b) COG-MAC

Fig. 7. Normalized energy cost with respect to the percentage of the observable WLAN spectrum activity (p_{CCA}).

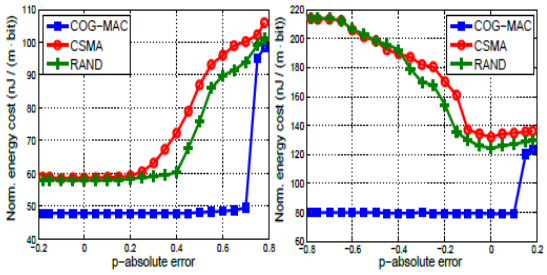

(a) $p = 0.2$ (b) $p = 0.8$

Fig. 8. Normalized energy cost with respect to the absolute of error in p-estimation, $[\hat{p} - p]$. $E\left[I^{(WS)}\right] = 36$msec ($\sigma = 0.025$).

load. For fixed packet sizes the effect of RTS/CTS handshakedepends on the WLAN load. Under high load values, that is, under short expected white-space durations, the increased performance due to efficient white-space discovery is limited, thus, it does not compensate for the additional overhead of the RTS/CTS mechanism.

3) Impact of the receiver observable load: Let us now investigate the effect of the observable load pR CCA on energy efficiency. Fig. 7 compares the CSMA and COG-MAC normalized energy cost as a function of pR CCA and for different p and E I(WS values. For the CSMA scheme (Fig. 7(a)) the energy cost increases monotonically with the observable load, since the interference-free time decreases. We can see similar trends for COG-MAC for low p values in Fig. 7(b). On the contrary, at high p value the COG-MAC energy cost decreases at high pR CCA, because in these scenarios COG-MAC can efficientlyfilter the short back-off periods. As a result, COG-MAC can provide energy efficient communication despite the limited sensing range, and can decrease the energy cost with up to 66% compared to CSMA.

4) Sensitivity to the model parameters: COG-MAC may not be able to use optimal packet size and

ISSN 2394-3777 (Print)
ISSN 2394-3785 (Online)
Available online at www.ijartet.com
International Journal of Advanced Research Trends in Engineering and Technology (IJARTET)
Vol. 3, Special Issue 24, April 2016

transmission distance due to imperfect WLAN Local View parameter estimation and due to the limited number of options that can be stored in the look-up table in the sensor memory. Here we study the effect of estimation errors on the energy efficiency. We evaluate the energy cost under a given WLAN activity
model realization, while COG-MAC variables are optimized in (13) considering erroneous p and values. (The results for the other model parameters are similar.) We present comparative results for CSMA and RAND. Fig. 8 shows the effect of the imperfect estimation of p, for low and high p values. We see that COG-MAC is not sensitive to estimation error, unless pis heavily overestimated, since the dual sensing filters out the back-off periods. CSMA and RAND, however, need to take the short back-off periods into account for the optimization, and therefore the imperfect estimation of p deteriorates their performance.

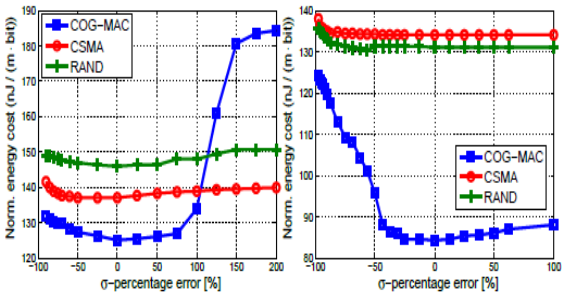

(a) $\sigma = 5 \cdot 10^{-3}$ (7msec) (b) $\sigma = 2 \cdot 10^{-2}$ (30msec)

Fig. 9. Normalized energy cost with respect to the percentage of error in σ-estimation, $[(\hat{\sigma} - \sigma)/\sigma]$. $p = 80\%$.

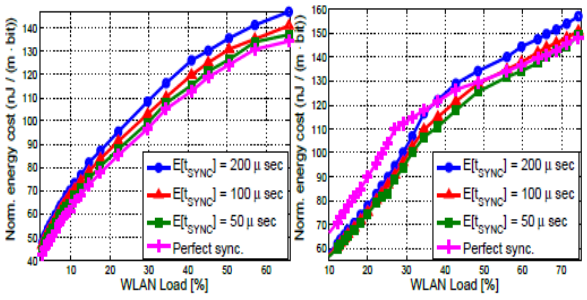

(a) $p = 20\%$ (b) $p = 80\%$

Fig. 10. Normalized communication energy cost with respect to increasing WLAN load (decreasing expected white-space duration), for different average synchronization offsets. $E\left[I^{(WS)}\right] = 60$msec.

Fig. 9 depicts the sensitivity of the performance on the
estimation of _, the shape parameter of the white space
distribution. For the considered scenario CSMA and RAND are not sensitive to estimation errors due to the high p value that makes the estimation of the actual WLAN white spaces less important. COG-MAC, however, transmits, primarily, in the white spaces, and therefore the over- and underestimation of _ leads to increased energy consumption. Still up to 50% error in estimating _ does not have significant effect on the energy cost. Based on [34], this level of accuracy can
be achieved by considering 100-1000 idle period samples. This in turn leads to an estimation time in the order of 1- 10 seconds, depending on the average lengths of the idle periods. The low sensitivity to estimation errors allows even the use of look-up tables with low granularity. These confirm that the proposed approach with local channel estimation and parameter optimization based cognitive access is a viable solution for sensor networks.

B. The effect of loose synchronization

In Fig. 10 we evaluate the energy cost of COG-MAC considering the case of imperfect synchronization of the TRand RR duty-cycles, based on the model in [33], Section VIB. We consider synchronization gaps uniformly distributed in (0; tmax
sync), E[tSYNC] = tmax sync=2. We show the effect of E[tSYNC] on the normalized COG-MAC energy cost as a function of the WLAN load, for low and high p values.
Since the shifted double sensing procedures require more time, synchronization gaps decrease the probability of successful handshake and reduce the interference-free time for packet transmission, and therefore can increase the energy cost, as demonstrated in Fig. 10(a). Fig. 10(b), however, shows that for high p values and low network load synchronization gaps may slightly improve protocol performance. The time-shift of the TR and RR sensing times increases the chance of detecting a WLAN transmission after undetected active period and back off time, and consequently increases the probability that the transmission happens in WLAN white space. All in all, synchronization offsets in the order of 100_sec have only a slight impact on the protocol performance.

VIII. A SIMULATION STUDY OF COG-MAC

The model-based evaluation in Section VII is subject to the two assumptions, i) the WLAN sources are uniformly distributed around the TR, and ii) the consecutive handshake and packet transmission

ISSN 2394-3777 (Print)
ISSN 2394-3785 (Online)
Available online at www.ijartet.com
International Journal of Advanced Research Trends in Engineering and Technology (IJARTET)
Vol. 3, Special Issue 24, April 2016

attempts in COG-MAC observe independent WLAN channel status. In addition, to simplify the derived analytical expressions, we made three approximations
in the model, in (10), (37) and (45). We present, here, a simulation study of COG-MAC, where the above assumptions and approximations are removed to see their effect on the protocol performance. Moreover, we evaluate COG-MAC in a multihop WSN.

A. Implementation and simulation scenario

We simulate the coexisting networks in the NS-Miracle framework [36]. The 802.11b-compliant NS-Miracle module is used for the WLAN nodes. For the WSN COG-MAC module we implemented model estimation, sensing, access control and packet reception model, as described in Sections III,V. WSN packet losses trigger retransmissions, occurring at consecutive duty-cycles of 50msec length. We consider a single WLAN AP area with a limited set of wireless terminals (WT), operating in the high SNR regime. We inject WLAN traffic by generating a packet stream that creates a sequence of idle and active periods that follow the proposed parameterized Global View model, and assign the packets to the WTs and the AP independently at random. To simulate a practical case we allocate 50% of the injected packets to the AP, assigning the rest, uniformly, at the WTs. We consider saturated buffer at the WSN TRs to minimize simulation time.

B. Model validation

We perform controlled experiments for a set of WLAN traffic parameter pairs (p;EI(WS)) as follows. For each experiment we first place a single RR sensor uniformly at random at a distance lower than RCCA from the AP and deploy 10 WTs uniformly at random outside the AR CCA. Thus the RR observes50% of the WLAN traffic (pR CCA = 0:5). We determine the optimal distance r_ and the packet size for possible ^pT CCA values by the optimal solution of (13), and place the TR randomly on circle with radius r_ around the RR. Clearly, this topology leads to non-uniform WLAN source distribution around TR. To achieve statistically meaningful averages we randomize the location of the RR and the 10 deployed WTs for 100 simulation runs within each experiment. Each simulation run terminates when the TR sensor completes the transmission of 500 packets, or, alternatively, when the simulation time exceeds 1000 seconds. The energy cost is calculated based on the number of the handshake and transmission attempts that each packet experiences.

Fig. 11 compares the simulation and analytic results forthe normalized energy cost with respect to p (Fig. 11(a))and with respect to increasing WLAN load _, by decreasingthe expected white space durations (Fig. 11(b)). Despite a slight overestimation of the communication energy cost by the analytic model, we can conclude that the model sufficiently captures the performance of COG-MAC. The analytically evaluated performance of CSMA is also plotted for the sake of comparison.
Fig. 11(c) shows the effect of the duration of the WSN duty-cycle on COG-MAC performance, and thus evaluates the modeling assumption of independent WLAN channel status at the consecutive dual sensing events. We consider the average per packet handshake and transmission attempts for duty-cycle periods from 15ms to 100ms. The WLAN load increases with p, while E[IWS] = 36msec. As the duty-cycle duration increases above 50msec, the simulated performance matches closely the analytic one, and for 100ms the performance difference is negligible, that is, the time between successive handshake or transmission attempts is long enough for COGMACto experience uncorrelated channel conditions. As the practical WSN duty-cycles are usually much longer than the ones we consider, we conclude that the assumption of independent WLAN status during consecutive COG-MAC cycles is practical.

C. Multihop COG-MAC performance analysis

Finally, we study the impact of COG-MAC on the energy efficiency of multihop WSN communication under WLAN interference. COG-MAC with energy optimized shortest path (SP) routing is compared to a benchmark solution with CSMA/CA and the widely accepted Collection Tree Protocol (CTP) [37], that finds the shortest path with the expected number of required transmissions per packet as the link weight. In COG-MAC the optimal packet sizes may differ for the links along a shortest path. To avoid the need for packet fragmentation, the packet size is chosen at the source node as the minimum of all optimal packet lengths along the path. Packet size is selected similarly for the benchmark system.
As shown in Fig. 12, we consider a square WSN grid with 5m inter-node distance, and a source and a destination node in the opposite corners. We place the WLAN AP in the center of the grid, and many of the WTs close to the AP, to generate a heterogeneous spectrum occupancy, with higher load around the center. We compare the performance of the two solutions for a constant _I(WS) and increasing p value, i.e., increasing WLAN load. Fig. 12(a) shows the transmission paths for two case studies with p =

ISSN 2394-3777 (Print)
ISSN 2394-3785 (Online)
Available online at www.ijartet.com
International Journal of Advanced Research Trends in Engineering and Technology (IJARTET)
Vol. 3, Special Issue 24, April 2016

0:2 and p = 0:8, respectively. For low p value, that is, low WLAN load the shortest paths are identical and traverse along the line connecting the source and destination node. For high load, however, the CSMA
based solution needs to avoid the area around the AP, andredirects the transmission path to the borders, where the WLAN interference is lower. At the same time COG-MAC can safely transmit along the diagonal. Fig. 12(b) gives the normalized energy and delivery delay per transmitted bit over the source-destination transmission path. The COG-MAC based solution outperforms the benchmark system, particularly when the back-off period percentage increases but the WLAN load is still moderate. We can conclude that COG-MAC leads to significant energy savings and lower delays in multihop WSNs, and, additionally, to optimal routes that are insensitive to WLAN load changes.

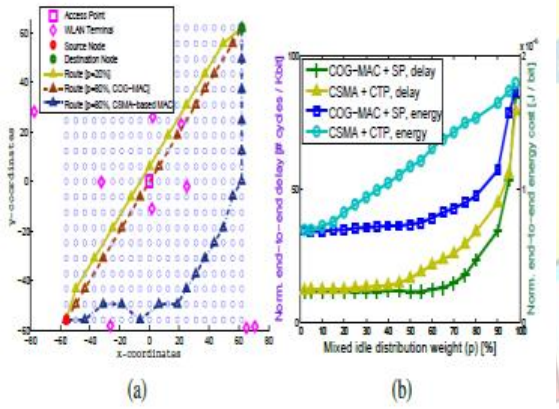

Fig. 12. (a) Topology and transmission paths for COG-MAC and CSMA-based cross-layer schemes under different percentage of WLAN back-off periods, p. (b) Normalized end-to-end energy cost per bit and end-to-end delay with respect to p. $\bar{I}^{(WS)} = 36ms$.

We consider a single WLAN AP area with a limited set of wireless terminals (WT), operating in the high SNR regime. We inject WLAN traffic by generating a
packet stream that creates a sequence of idle and active periods that follow the proposed parameterized Global View model, and assign the packets to the WTs and the AP independently at random. To simulate a practical case we allocate 50% of the injected packets to the AP, assigning the rest, uniformly, at the WTs. We consider saturated buffer at the WSN TRs to minimize simulation time.

The COG-MAC based solution outperforms the benchmark system, particularly when the back-off period percentage increases but the WLAN load is still moderate. We can conclude that COG-MAC leads to significant energy savings and lower delays in multihop WSNs, and, additionally, to optimal routes that are insensitive to WLAN load changes.

ISSN 2394-3777 (Print)
ISSN 2394-3785 (Online)
Available online at www.ijartet.com
International Journal of Advanced Research Trends in Engineering and Technology (IJARTET)
Vol. 3, Special Issue 24, April 2016

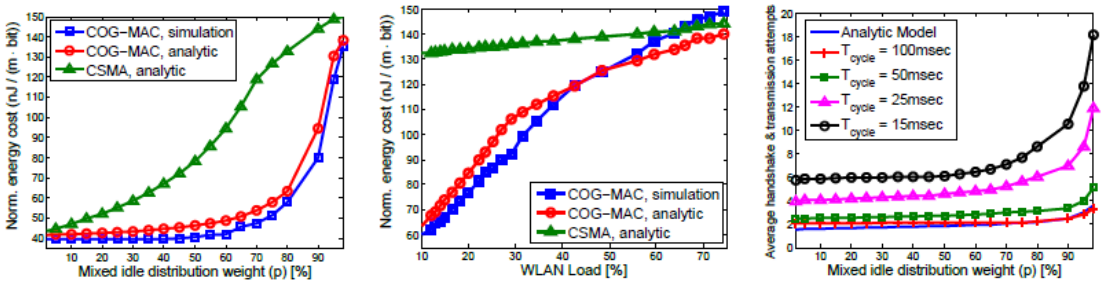

(a) $\bar{I}^{(WS)} = 60$msec (b) $p = 0.8$ (c)

Fig. 11. (a), (b) Comparison between numerical and simulation results for COG-MAC under various p, σ parametrization sets and (c) average handshake and transmission attempts with respect to increasing percentage of back-off periods, parameterized by the WSN duty-cycle duration.

IX. CONCLUSION

In this paper we proposed COG-MAC, a cognitive MAC scheme for energy efficient WSN operation under WLAN coexistence. The proposed scheme is based on controlling the interference from the coexisting WLAN by predicting its behavior with a smart channel sensing mechanism that takes into consideration the WLAN channel usage model. Energy cost minimization is achieved by optimizing the WSN single hop transmission distance and packet length, based on the estimated parameters of the WLAN channel usage model. To solve the optimization problem we derived an analytic model for the successful single-hop WSN packet communication. Through numerical evaluation we showed that COG-MAC significantly outperforms other MAC protocols, especially in case of severe WLAN interference. The evaluation also revealed that both COG-MAC optimization of packet size and transmission distance and smart channel sensing are key mechanisms for increasing energy efficiency. We also presented simulation results to demonstrate the accuracy of the analytic modeland to show that COG-MAC achieves significant gains even in multihop environment. Consequently, COG-MAC provides a distributed solution that exploits existing functionalities available in current commercial sensor hardware, and archives energy-efficient communications in the presence of coexisting WLAN networks.

REFERENCES

[1] S. Pollin, I. Tan, B. Hodge, C. Chun, and A. Bahai, "Harmful coexistencebetween 802.15.4 and 802.11: A measurement-based study," in Proceedings of the 3rd International Conference on Cognitive Radio Oriented Wireless Networks and Communications, pp. 1–6, May 2008.

[2] S. Geirhofer, L. Tong, and B. Sadler, "Dynamic spectrum access in the time domain: Modeling and exploiting white space," IEEE Communications Magazine, vol. 45, pp. 66 –72, May 2007.

[3] J. Al-Karaki and A. Kamal, "Routing techniques in wireless sensor networks: a survey," IEEE Wireless Communications, vol. 11, pp. 6 – 28, Dec. 2004.

[4] A. Bachir, M. Dohler, T. Watteyne, and K. Leung, "MAC essentials for Wireless Sensor Networks," IEEE Communications Surveys Tutorials, vol. 12, no. 2, pp. 222–248, 2010.

[5] P. Lin, C. Qiao, and X. Wang, "Medium access control with a dynamic duty cycle for sensor networks," in IEEE Wireless Communications and Networking Conference (WCNC), vol. 3, March 2004.

[6] M. Buettner, G. V. Yee, E. Anderson, and R. Han, "X-MAC: a short Preamble MAC Protocol for Duty-Cycled Wireless Sensor Networks," in Proceedings of the 4th International Conference on Embedded Networked Sensor Systems, SenSys'06, pp. 307–320, ACM, 2006.

[7]Christo Ananth, T.Rashmi Anns, R.K.Shunmuga Priya, K.Mala, "Delay-Aware Data Collection Network Structure For WSN", International Journal of Advanced Research in Biology, Ecology, Science and Technology (IJARBEST), Volume 1,Special Issue 2 - November 2015, pp.17-21

[8] M. Di Francesco, G. Anastasi, M. Conti, S. Das, and V. Neri, "Reliabilityand Energy-Efficiency in IEEE 802.15.4/ZigBee Sensor Networks: An Adaptive and Cross-Layer Approach," IEEE Journal on Selected Areas in Communications, vol. 29, pp. 1508–1524, Sep. 2011.

[9] A. Camillò, M. Nati, C. Petrioli, M. Rossi, and M. Zorzi, "Iris: Integrated data gathering and interest dissemination system for wireless sensor networks," Ad Hoc Networks, vol. 11, no. 2, pp. 654–671, 2013.

[10] C. Petrioli, D. Spenza, P. Tommasino, and A. Trifiletti, "A novel wake-up receiver with addressing capability for wireless sensor nodes," in Distributed Computing in Sensor Systems (DCOSS), 2014 IEEE International Conference on, pp. 18–25, May 2014.

[11] L. Lo Bello and E. Toscano, "Coexistence Issues of Multiple Colocated IEEE 802.15.4/ZigBee Networks Running on Adjacent Radio Channels in Industrial Environments," IEEE Transactions on Industrial Informatics, vol. 5, pp. 157–167, May 2009.

[12] L. Angrisani, M. Bertocco, D. Fortin, and A. Sona, "Experimentalstudy of coexistence issues between IEEE 802.11b and IEEE 802.15.4Wireless Networks," IEEE Transactions on Instrumentation and Measurement,vol. 57, pp. 1514–1523, Aug. 2008.

[13] S. Y. Shin, H. S. Park, S. Choi, and W. H. Kwon, "Packet error rateanalysis of ZigBee under WLAN and Bluetooth Interferences," IEEETransactions on Wireless Comm., vol. 6, no. 8, pp. 28252830, 2007.

14] M. Hanninen, J. Suhonen, T. Hamalainen, and M. Hannikainen,

ISSN 2394-3777 (Print)
ISSN 2394-3785 (Online)
Available online at www.ijartet.com
International Journal of Advanced Research Trends in Engineering and Technology (IJARTET)
Vol. 3, Special Issue 24, April 2016

"Link quality-based channel selection for resource constrained WSNs," Springer Advances in Grid and Pervasive Computing, vol. 6646, pp. 254–263, 2011.

[15] K. il Hwang, S.-S. Yeo, and J. H. Park, "Adaptive multi-channel utilization scheme for coexistence of IEEE 802.15.4 LR-WPAN with other interfering systems," in Proceedings of the 11th IEEE International Conference on High Performance Computing and Communications, 2009. HPCC'09, pp. 297–304, Jun. 2009.

[16] J. Ansari and P. Mähönen, "Channel selection in spectrum agile and cognitive mac protocols for wireless sensor networks," in Proceedings of the 8th ACM international workshop on Mobility management and wireless access, ACM MobiWac'10, pp. 83–90, ACM, 2010.

[17] H. Rahul, N. Kushman, D. Katabi, C. Sodini, and F. Edalat, "Learning to share: Narrowband-friendly wideband networks," SIGCOMM Comput. Commun. Rev., vol. 38, pp. 147–158, Aug. 2008.

[18] K. Chowdhury and I. Akyildiz, "Interferer Classification, Channel Selection and Transmission Adaptation for Wireless Sensor Networks," in Proceedings of IEEE International Conference on Communications, pp. 1–5, June 2009.

[19] Y. Wu, G. Zhou, and J. Stankovic, "ACR: Active Collision Recovery in Dense Wireless Sensor Networks," in Proceedings of IEEE International Conference on Computer Communications, pp. 1–9, Mar. 2010.

[20] C. Liang, N. Priyantha, J. Liu, and A. Terzis, "Surviving Wi-Fi interference in low power ZigBee networks," in Proceedings of the 8th ACM Conference on Embedded Networked Sensor Systems, pp. 309– 322, 2010.

[21] P. Rathod, O. Dabeer, A. Karandikar, and A. Sahoo, "Characterizing the exit process of a non-saturated ieee 802.11 wireless network," in MobiHoc, pp. 249–258, 2009.

[22] J. Misic and V. Misic, "Characterization of idle periods in IEEE
802.11e networks," in Proceedings of IEEE Wireless Communications and Networking Conference (WCNC), pp. 1004–1009, Mar. 2011.

[23] S. Geirhofer, L. Tong, and B. M. Sadler, "Cognitive medium access: Constraining interference based on experimental models," IEEE Selected Areas in Communications, vol. 26, no. 1, 2008.

[24] L. Stabellini, "Quantifying and modeling spectrum opportunities in a real wireless environment," in Proceedings of Wireless Communications and Networking Conference (WCNC), pp. 1–6, Apr. 2010.

[25] I. Glaropoulos, A. Vizcaino Luna, V. Fodor, and M. Papadopouli,"Closing the gap between traffic workload and channel occupancy models for 802.11 networks," Ad Hoc Netw., vol. 21, pp. 60–83, Oct. 2014.

[26] J. Huang, G. Xing, G. Zhou, and R. Zhou, "Beyond Co-existence; Exploiting WiFi White Space for ZigBee Performance Assurance," in Proceedings of IEEE International Conference on Netw.Protocols, 2010.

[27] S. Geirhofer, J. Z. Sun, L. Tong, and B. M. Sadler, "Cognitive frequency hopping based on interference prediction: theory and experimental results," ACM SIGMOBILE Mob. Comput.Commun. Rev., vol. 13, pp. 49–61, Sep. 2009.

[28] I. Glaropoulos, V. Fodor, L. Pescosolido, and C. Petrioli, "Cognitive WSN transmission control for energy efficiency under WLAN coexistence,"in Proceedings of the 6th International Conference on Cognitive Radio Oriented Wireless Networks and Communications, Jun. 2011.

[29] X. Liu, S. Zhang, J. Wang, J. Cao, and B. Xiao, "Anchor supervised distance estimation in anisotropic wireless sensor networks," in Proceedings of IEEE Wireless Communications and Networking Conference, pp. 938–943, Mar. 2011.

[30] "2.4GHz IEEE 802.15.4 / ZigBee-ready RF Transceiver," tech. rep., Texas Instruments, 2008